energy&fuels

pubs.acs.org/EF

Article

Harvesting Electrical Power during Carbon Capture using Various Amine Solvents

Trevor J. Kalkus, Caitlin J. Shanahan, Jansie Smart, Ali Coskun, and Michael Mayer*

Cite This: *Energy Fuels* 2022, 36, 11051−11061

Read Online

ACCESS | Metrics & More | Article Recommendations | Supporting Information

ABSTRACT: There exists an urgent demand for the advancement of technologies that reduce and capture carbon dioxide (CO_2) emissions to mitigate anthropogenic contributions to climate change. This paper compares the maximum power densities achieved from the combination of reverse electrodialysis (RED) with carbon capture (CC) using various CC solvents. Carbon capture reverse electrodialysis (CCRED) harvests energy from the salinity gradients generated from the reaction of CO_2 with specific solvents, generally amines. To eliminate the requirement of freshwater as an external resource, we took advantage of a semiclosed system that would allow the inputs to be industrial emissions and heat and the outputs to be electrical power, clean emissions, and captured CO_2. We assessed the power density that can be attained using CCRED with five commonly studied CC solvents: monoethanolamine (MEA), diethanolamine (DEA), *N*-methyldiethanolamine (MDEA), 2-amino-2-methyl-2-propanol (AMP), and ammonia. We achieved the highest power density, 0.94 W m^{-2} $cell^{-1}$, using ammonia. This work provides a foundation for future iterations of CCRED that may help to incentivize adoption of CC technology.

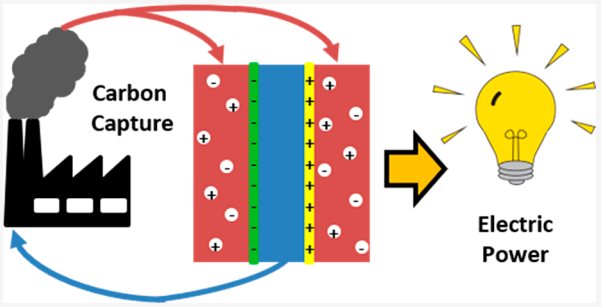

1. INTRODUCTION

Anthropogenic emissions of carbon dioxide (CO_2) and other greenhouse gases contribute significantly to climate change, influencing many environmental and biological phenomena, including, but not limited to, extreme weather patterns and ocean acidification.[1,2] A large variety of sustainable technologies have been introduced to reduce the dependence on the combustion of fossil fuels.[1] These efforts include green energy technologies that harvest electrical power from solar power, wind power, geothermal heat, and other renewable resources.[3] Although these technologies have been improving rapidly, they are still insufficient to address the current crisis, especially as energy demands continue to rise.[4]

Another category of sustainable energy involves harvesting energy from salinity gradients and has been labeled 'blue energy'.[5,6] Reverse electrodialysis (RED) and pressure retarded osmosis (PRO) are the most common implementations of blue energy.[5,6] The process of PRO uses a semipermeable membrane to separate two solutions with different salinities. As water migrates to the higher salinity solution, the resulting pressure is used to generate electrical power in a turbine.[7−9] The greatest limitation of PRO is the development of supported semipermeable membranes with high permeability to water.[10,11] When harvesting energy from the mixing of freshwater and seawater, RED achieves higher power density and higher energy recovery than PRO, and improvements to RED systems have been more successful than improvements to PRO.[10−12] The process of RED uses charge-selective membranes to separate a high-salinity solution (traditionally seawater) and a low-salinity solution (traditionally freshwater).[13−15] As ions from the high-salinity solution diffuse to the low-salinity solution, charge selective membranes restrict the diffusion of cations to one direction and the diffusion of anions to the opposite direction (Figure 1a).[13−15] The resulting separation of charges creates a potential difference across each charge-selective membrane, and the sum of these potentials in series results in the total potential difference across the entire device.[13−15] Although a significant amount of energy can theoretically be made available while large volumes of freshwater and saltwater mix,[16] access to this process is limited to specific geographic areas.[17] The use of concentrated brines from some industrial activities can also provide a source of high-salinity solutions and can even increase the power that can be produced using RED.[18] The development of RED, however, has not yet resulted in a cost-efficient method for providing renewable energy.[15,17,19] A significant reason RED falls short of expectations is the fouling that occurs on the charge-selective membranes when using natural solutions.[20,21] In pilot-scale tests of RED, artificial solutions provided nearly

Received: July 7, 2022
Revised: August 18, 2022
Published: August 31, 2022

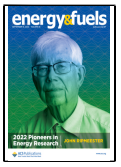

https://doi.org/10.1021/acs.energyfuels.2c02279
Energy Fuels 2022, 36, 11051−11061

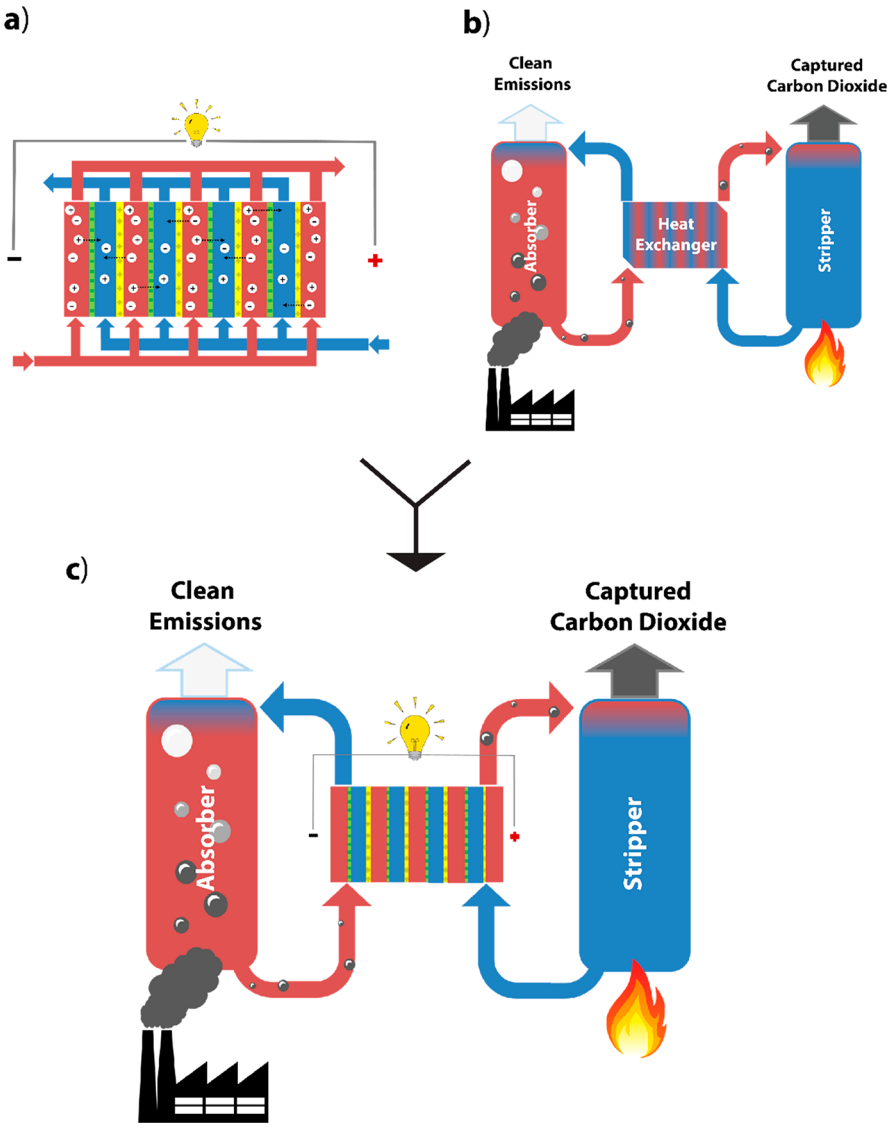

Figure 1. Illustration depicting the concept of combining carbon capture (CC) and reverse electrodialysis (RED). (a) Depiction of RED. Solutions of low- and high-salinity flow past each other separated only by charge-selective membranes in a repeating pattern: high-salinity solution (red), cation-selective membrane (green), low-salinity solution (blue), and anion-selective membrane (yellow). The controlled diffusion of ions leads to a separation of charges, generating a potential difference across each charge selective membrane. This potential difference can be harvested in the form of electrical power. (b) Depiction of solvent-based CC. The CO_2 in industrial emissions reacts with the CC solvent in the absorber, generating the rich solution. After CO_2 removal, only clean emissions are released, and the CO_2-rich solution is delivered to the stripper. In the stripping process, the rich solution is heated to release CO_2 gas, which is then sequestered or utilized, resulting in the regeneration of the lean solution, which is delivered back to the absorber. To conserve energy, the solutions pass through a heat exchanger as they circulated so that the heated lean solution will transfer heat to the rich solution before entering the stripper. (c) By using the lean and rich solutions as the low- and high-salinity solutions for RED, the infrastructure already established for heat exchange during the CC process theoretically provides the conditions for the implementation of CCRED, which similarly requires the regular circulation of both solutions in close contact.

double the power density compared to natural solutions with the same conductivity.[22]

The development and adoption of sustainable technologies has been insufficient to meet the goals for the reduction of carbon emissions.[4,23] For these reasons, many scientists, nations, and industries expect that carbon capture (CC) technology will be essential for effectively reducing atmospheric concentrations of greenhouse gases.[24−26] One of the most developed and studied methods for CC is chemisorption, which often involves the use of an amine solvent that reacts with the CO_2 (Figure 1b).[25,27,27−29] The solvent solution that contains little to no CO_2 is referred to as a CO_2-lean solution (henceforth a lean solution), and the solvent solution that has reacted with and absorbed CO_2 is referred to as a CO_2-rich solution (henceforth a rich solution). To regenerate the lean solution after it has been loaded with CO_2, the rich solution is heated to recover the CO_2 via the stripping process.[25,27] The pure CO_2 is then stored or utilized, and the CC solution can be reused.[24,30,31] The energetic cost of this solvent regeneration, however, is a primary reason that CC technology is not more widely adopted.[27,28,32−34] For example, the energy necessary to regenerate solvent when this method is used to clean emissions from a coal-burning power plant can increase the energy requirements of the plant by 25−40%.[35] The energetic cost, and the corresponding monetary cost, disincentivizes the implementation of CC technology.[35] To conserve energy,

https://doi.org/10.1021/acs.energyfuels.2c02279
Energy Fuels 2022, 36, 11051−11061

implementations of solvent-based CC use a heat exchanger between the CO_2 absorption process, which generally benefits from a low-temperature solution, and the CO_2 stripping process, which requires high temperatures (Figure 1b).[28] The energetic costs of CC may also be reduced by using CC solvents that require less energy to be regenerated.[27,28,32,35]

To generate value from carbon utilization to motivate CC, large amounts of capital have been invested into accelerating technologies that utilize CO_2.[36,37] Kim et al. recently suggested that value can be created during the CC process by harvesting electric power using RED.[23] They demonstrated the integration of CC and RED, an approach labeled carbon capture reverse electrodialysis (CCRED), and suggested that this combination can address shortcomings of both individual processes.[23] Because the amine solutions that are used for CCRED are not collected from natural sources, membrane fouling may be less likely than when using freshwater and seawater.[20] Additionally, the electrical power generated by RED can be used to help reduce the energetic costs of CC.[23] Although CCRED is unlikely to address all of the energy requirements of CC, the reduced cost can contribute to increasing the economic motivation for implementing CC technology.

The reaction of CO_2 with an amine CC solvent generates ionic species (eqs 1−5). This increase in salinity allows for the rich solution to be used as a high-salinity solution for RED.[23] Kim et al. used distilled water as the low-salinity solution for their CCRED device.[23] Distilled water is an external resource that would be required in continuous supply, and it would become polluted with the CC solvent during the CCRED process, requiring additional precautions for disposal in an environmentally safe way. By using distilled water as the low-salinity solution, the CCRED design proposed by Kim et al. would likely not be practical for implementation in full-scale CC systems.[23] Recently, we demonstrated that lean CC solutions can be used as the low-salinity solution instead of distilled water.[38] In principle, this design allows the amine solutions to remain in a closed system with flue gas and heat as inputs and pure CO_2, treated emissions, and electrical energy as outputs. Additionally, because the conductivity of the lean solution is higher than that of distilled water, the use of the lean solution reduces the internal resistance of the device and increases power density.[38] Most significantly, the implementation of CCRED in existing CC infrastructure may be relatively seamless considering that the heat exchanger already provides a step in the process where the lean and rich solutions flow past each other in close contact (Figure 1c).

In this work, we focused on analyzing a feature unique to the combination of CC and RED: the difference in power density that results from using different CC solvents. A variety of CC solvents have been investigated in an attempt to find a best candidate for industrial scale CC.[27,29,32] The benchmark for CC solvents has been monoethanolamine (MEA) due to its rapid reaction kinetics with CO_2, ensuring efficient CO_2 capture.[27,32,39,40] For this reason, we used MEA in previous work when we demonstrated a novel CCRED design that could produce electrical power from the ion gradient generated when capturing CO_2 in breath.[38] In the CCRED device presented by Kim et al., the authors used *N*-methyldiethanolamine (MDEA) because the energy required to regenerate MDEA is lower than that required for MEA.[23] A number of other CC solvents, including diethanolamine (DEA), 2-amino-2-methyl-2-propanol (AMP), and ammonia, as well as mixes of CC solvents have been proposed to strike the balance between fast reaction kinetics and lowering the regeneration energy cost.[27−29,29,32,33,41−45]

Ammonia is a particularly interesting candidate for CCRED because it has already been demonstrated in thermolytic RED systems designed to generate energy from low-grade waste heat.[46−49] Because ammonium bicarbonate will evaporate out of solution as ammonia and CO_2 gas at relatively low temperatures (around 60 °C), waste heat from some industrial processes is sufficient to remove these ions.[49] In a completely closed system, an ammonium bicarbonate solution can be used as the high-salinity solution, and low-grade heat can remove the ions to regenerate a low-salinity solution.[49] In principle, the gases and solution could be recycled indefinitely to continuously harvest power from waste heat.[46−49]

When using different CC solvents, the reaction with CO_2 produces different ionic species; sterically hindered amines become protonated and CO_2 forms bicarbonate with water molecules, whereas unhindered amines (MEA and DEA) react directly with CO_2 to form carbamates in addition to generating protonated species and bicarbonate (eqs 1−5).[23,27,45] We have previously demonstrated that the composition of ionic species in salinity gradient power sources impacts the resulting power density.[38,50] Here, we directly compare different CC solvents (MEA, DEA, MDEA, AMP, and ammonia) in the same lab-scale CCRED device and demonstrate that ammonia achieved the highest power density, reaching nearly 1 W m^{-2} $cell^{-1}$. Ultimately, these results suggest that CCRED could potentially contribute to economically motivating adoption of CC technology.

2. MATERIALS AND METHODS

2.1. Materials. All chemicals, monoethanolamine (MEA), diethanolamine (DEA), *N*-methyldiethanolamine (MDEA), 2-amino-2-methyl-2-propanol (AMP), 32% ammonia solution, potassium carbonate, potassium chloride, potassium hexacyanoferrate (II) and potassium hexacyanoferrate (III), were purchased from Sigma-Aldrich. Silicone rubber sheets (0.5 mm thickness) were ordered from Vibraplast AG. We purchased charge selective membranes, Fumasep FKB-PK-130 (100−130 μm thick, polyether ether ketone (PK) reinforced, cation exchange), FKS-50 (45−55 μm thick, no polymer reinforcement, cation exchange), FAB-PK-130 (100−130 μm thick, PK reinforced, anion exchange), and FAS-50 (45−55 μm thick, no polymer reinforcement, anion exchange) membranes, from Fumatech BWT GmbH. Fumatech specifies that these membranes have a selectivity of 92−99% and are stable within the pH 1−14 range. We made spacers using SEFAR PETEX 07-120/50 mesh (120 μm mesh opening, 50% open area, 80 μm thickness), and some preliminary trials used NITEX 03-170/54 (170 μm mesh opening, 54% open area, 100 μm thickness), from SEFAR AG. We fabricated the electrode compartments from acrylic material at the machine shop at the University of Fribourg, Switzerland. We provided the design modeled in Microsoft 3D builder (Supporting Information, Figure S4). The company SGL Carbon GmbH provided sigracell graphite battery felt, GFD, with 4.6 mm thickness. We purchased platinum wire (0.3 mm diameter) from Alfa Aesar. We purified water to 18.2 MΩ cm with a PURELAB Flex II purifier (ELGA LabWater, Veolia).

2.2. Constructing the Electrode Compartments. We soldered a platinum current collecting wire to an electrical pin and glued it using epoxy in the center of each electrode compartment, with the platinum wire inside the compartment and the pin providing access outside the compartment. We embedded the platinum wire in graphite felt that we cut to a circular area of 19.6 cm to fill the electrode compartment. We spread an extremely thin layer of Dow Corning high vacuum grease on the acrylic surface to aid in creating a seal with a silicone layer that served as a gasket for holding a CEM in

https://doi.org/10.1021/acs.energyfuels.2c02279
Energy Fuels 2022, 36, 11051−11061

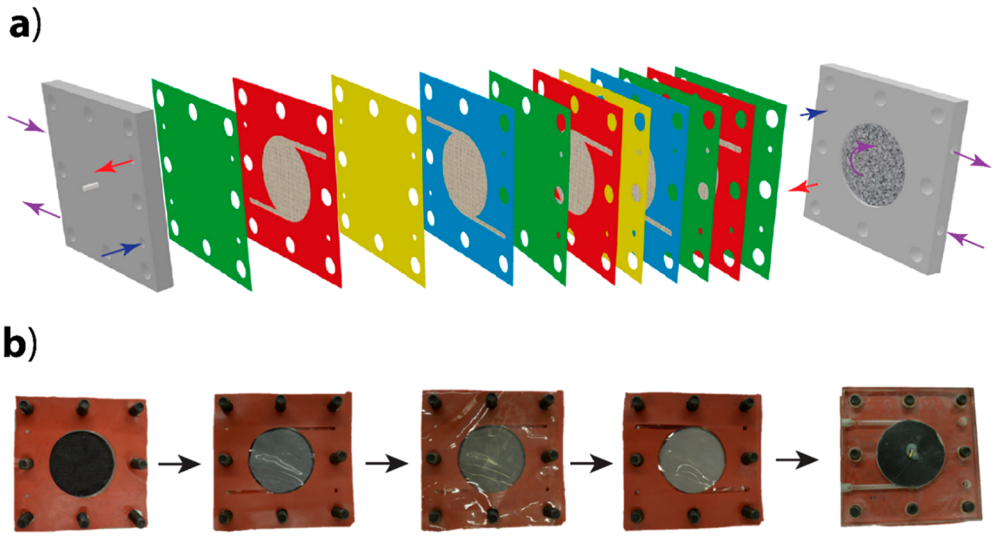

Figure 2. Design of the CCRED device. (a) 3D representation of the complete device. The end pieces (gray) contain the graphite felt electrodes (marble pattern) and a platinum wire to collect current. An electrode solution containing potassium hexacyanoferrate (purple arrows) is circulated separately through both terminal compartments at the same rate as the lean and rich solutions circulate through their respective compartments. Cation-exchange membranes (green) separate the electrode compartments. The repeating pattern that composes a single CCRED cell is rich compartment (red), anion-exchange membrane (yellow), lean compartment (blue), and cation-exchange membrane (green). Spacers within the rich and lean compartments are indicated by a mesh texture. The rich solution (red arrow) flows into an inlet at the bottom of one end piece, through the rich compartments, and out an outlet at the top of the other end piece. The lean solution (blue arrow) flows in the opposite direction into an inlet at the bottom of one end piece, through the lean compartments, and out an outlet at the top of the other end piece. Eight holes around the edges of all the compartments allow for bolts that hold the CCRED device together. (b) Pictures of the CCRED device at certain stages as it is being assembled. From left to right: the end piece with a silicone gasket and the graphite felt, the first cation-exchange membrane and rich compartment with spacer, the anion exchange membrane stacked on the previous layer, the lean compartment with spacer, and the final assembly with the second end piece.

place to separate the electrode compartment from the neighboring high-salinity compartment. This CEM prevented anions from the electrolyte solution in the electrode compartment from diffusing to other compartments. The electrolyte solution consisted of 0.05 M potassium hexacyanoferrate (II), 0.05 M potassium hexacyanoferrate (III), and 0.5 M potassium chloride. We chose to use the redox reaction of a hexacyanoferrate solution with graphite to convert the ionic current to electric current based on previous assessment of electrode assemblies for RED done by Veerman et al.[51] The standard electrode potential of hexacyanoferrate ($[Fe(CN)6]^{4-}/[Fe(CN)6]^{3-}$) is $E^0 = 0.356$ V.[51] However, because opposite reactions are occurring at the two electrodes, the Nernst potential of reduction on the cathode is counterbalanced by oxidization on the anode, resulting in a net zero contribution to the overall measured potential.[51] We circulated the electrolyte solution separately through the electrode compartments at the same flow rate as the high-salinity and low-salinity solutions. We used the same electrode setup on both ends of the device.

2.3. Constructing the Reverse Electrodialysis Device. The CCRED device was assembled using 0.5 mm thick silicone gaskets, Fumasep FKS-50 as the cation exchange membrane, Fumasep FAS-50 as the anion exchange membrane, and 80 μm thick spacers with 50% open area. The gaskets created a circular effective membrane area of 19.63 cm^2 for each membrane. We created the spacers to fit within the gasket so that they occupy each compartment as well as the channels leading to each compartment. We cut the shapes for the silicone gasket material (which formed the low-salinity and high-salinity compartments), the charge-selective membranes, and the spacers using a Cricut Maker cutting machine (Cricut Inc.). The cutting patterns used can be accessed by the link provided in the Supporting Information.

Assembling the components proceeded as follows: After the CEM that contained the electrode compartment, a silicone gasket forming a high-salinity compartment was added with a spacer inside the channels and the compartment. We then added an AEM, followed by a silicone gasket forming a low-salinity compartment with a spacer inside the channels and compartment and then a CEM. We repeated this pattern one more time for a total of two cells. We completed the device with the second electrode compartment. We placed the high- and low-salinity gaskets in opposite orientations so that they lead to the appropriate input and output channels (Figure 2). Eight bolts, placed through holes on the sides and corners of the device, held the device together tightly and evenly.

We implemented a Glison Minipuls 3 peristaltic pump to circulate the solutions through the compartments. We used a flow rate of approximately 7.6 mL min^{-1} $cell^{-1}$ for all experiments unless stated otherwise (Supporting Information, Figure S2). For each trial, we first made the lean solution for each solvent at the desired concentration (3.28 M MEA, 3.28 M DEA, 1.74 M MDEA, 1.74 M AMP, 1.74 M ammonia, 3 M ammonia). We then separated half of the lean solution and saturated it with CO_2 until the pH stabilized to generate the rich solution. We used four separate channels on the peristaltic pump to simultaneously push the desired lean and rich solution through their respective channels as well as push the electrode solution through each electrode compartment.

We used the peristaltic pump to rinse the CCRED device with a 1.74 M KCl solution and a 12 mM KCl solution in the rich and lean compartments, respectively, between uses to remove traces of CC solutions and refresh the membranes.

2.4. Characterizing Power. As the rich and lean solutions of the desired solvent traveled through the CCRED device, we measured voltage and current using a Keithley 2400 SourceMeter connected to the electrical pins on the end plates. We allowed for values to stabilize before being recorded (generally around 2 min). We used the measurements of open circuit voltage, voltage with a 99 Ω load, and short circuit current to characterize power density. We normalized power density by cell, which consists of one membrane pair.

2.5. Estimating Ammonia Concentration. We found that the aqueous ammonia stock solution (32%) was most likely over the saturation limit at our altitude (610 m) and temperature range. After generating rich solutions of various concentrations, we correlated the measured conductivities with reported conductivities of ammonium

https://doi.org/10.1021/acs.energyfuels.2c02279
Energy Fuels 2022, 36, 11051−11061

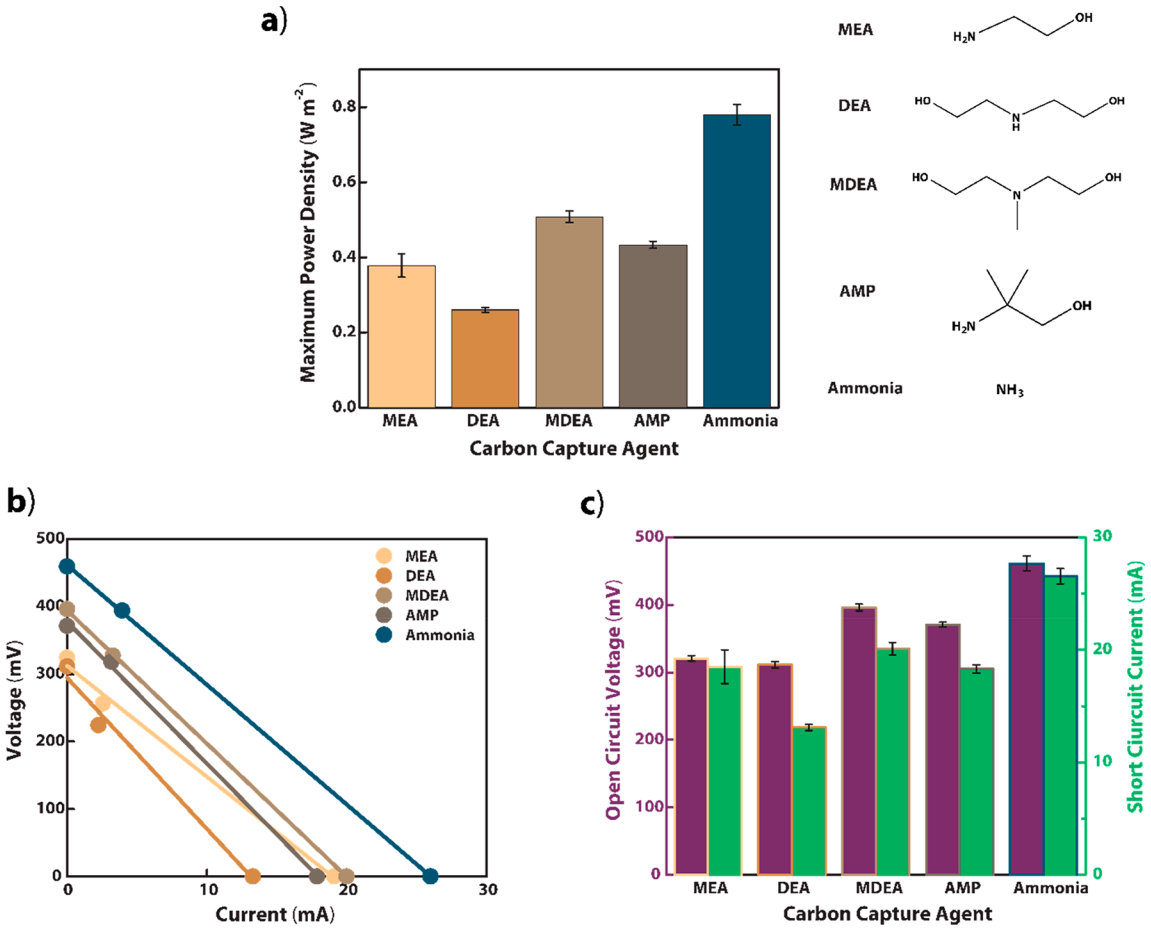

Figure 3. Power characteristics of CCRED using different CC solvents. (a) Maximum power density from CCRED using various CC solvents. The chemical structures of the different CC solvents are shown to the right. (b) Representative current−voltage curve for each CC solvent. A resistive load of 99 Ω was used to acquire the middle datum for each CC solvent. Lines are linear fits. (c) Open circuit voltage and short circuit current of CCRED for each CC solvent.

bicarbonate in the literature to determine the concentration.[49] Based on the conductivities of the generated solutions, we estimated that the stock solution was approximately 13.77 M ammonia. To limit the loss of ammonia as a gas, all ammonia solutions were kept in sealed containers when not being used, and CO_2 was added to the ammonia solution at a slow rate to prevent aggressive bubbling that might allow gas be stripped out of the solution.

2.6. Measurements of pH and Conductivity. We measured pH using a calibrated PH8500-SB portable pH meter for strong basic solutions (purchased from Apera Instruments). We measured conductivity using a Seven Compact Duo pH/Conductivity meter from Mettler Toledo.

2.7. Addition of CO_2. We sourced pure CO_2 from a pressurized tank provided by Carbagas AG, and we regulated the pressure to 1 bar. We dispersed CO_2 gas into the desired CC solutions using a gas dispersion tube with a porous fritted glass tip, 4−8 μm porosity, produced by Ace Glass, Inc. and purchased from Sigma-Aldrich. A Supelco Rotameter with a needle valve (flow range 0−110 mL min^{-1}) was purchased from Sigma-Aldrich controlled CO_2 gas flow rate. We added CO_2 until the pH stabilized, indicating maximum carbon loading.

2.8. Statistical Analysis. The data are presented as the mean ± standard deviation (SD), with a sample size of n = 3 unless stated otherwise. We propagated uncertainty accordingly when we used measured values in calculations.

3. RESULTS AND DISCUSSION

3.1. Design of the Carbon Capture Reverse Electrodialysis Device. When designing a CCRED system, a variety of parameters influence power density (Supporting Information, Figures S1 and S2). For example, reducing the intermembrane distance (the distance that separates the charge-selective membranes) results in a higher power density due to the reduction of internal resistance.[12,52] As the membranes are designed closer together, however, it is more likely that they may bulge and come into contact, especially because of the osmotic pressure caused by the different salinities. To prevent the membranes from touching, mesh spacers are often used in the compartments.[53−56] We modeled the CCRED device in this work after the one presented by Kim et al. (Figure 2).[23,57] Kim et al. also demonstrated that open circuit voltage increases as the flow rate of the low- and high-salinity solutions increases because mixing is minimized and the salinity gradient is maintained.[57] We similarly found that faster flow rates resulted in higher open circuit voltage (Supporting Information, Figure S2).

3.2. Power Density Generated by Different CC Solvents. In order to compare the performance of different CC solvents, namely, MEA, DEA, MDEA, AMP, and ammonia, using the CCRED device shown in Figure 2, we sought to generate comparable salinity gradients using each CC solvent because the voltage and power produced by RED

https://doi.org/10.1021/acs.energyfuels.2c02279
Energy Fuels 2022, 36, 11051−11061

Table 1. Conductivity of the Lean and Rich Solutions

CC solvent	solvent concentration (M)	conductivity of lean solution (mS cm^{-1})	pH of lean solution	conductivity of rich solution (mS cm^{-1})	pH of rich solution
MEA	3.28	1.086	12.2	49.70	7.8
DEA	3.28	0.9603	11.7	15.07	7.9
MDEA	1.74	0.2871	11.4	34.69	7.5
AMP	1.74	0.9756	12.2	32.15	7.9
ammonia	1.74	1.271	11.8	104.4	7.9

relates to the difference in ion concentration between solutions (Supporting Information, Sections S4−S6). The CC solvents react with CO_2 differently and have different theoretical maximum carbon loadings. MEA and DEA react to form relatively stable carbamates:[23,27,43,58,59]

$$2MEA + CO_2 \rightarrow MEACOO^- + MEAH^+ \quad (1)$$

$$2DEA + CO_2 \rightarrow DEACOO^- + DEAH^+ \quad (2)$$

According to these reactions, it is expected that MEA and DEA (a primary and secondary amine respectively) would be able to capture approximately 0.5 mol of CO_2 per mol of amine. Sterically hindered amines and ammonia, on the contrary, do not form stable carbamate species. For this reason, the reaction produces a protonated species and a bicarbonate:[23,29,43−45,60]

$$MDEA + CO_2 + H_2O \rightarrow HCO_3^- + MDEAH^+ \quad (3)$$

$$AMP + CO_2 + H_2O \rightarrow HCO_3^- + AMPH^+ \quad (4)$$

$$NH_3 + CO_2 + H_2O \rightarrow HCO_3^- + NH_4^+ \quad (5)$$

Using MDEA, AMP, or ammonia, the theoretical carbon loading can reach 1 mol of CO_2 per mol of hindered amine or ammonia[23,29,43−45] (Figure 3 shows the chemical structures). We expected twice as many ions to form when capturing CO_2 with MDEA, AMP, or ammonia than when using the same concentration of MEA or DEA. We used eqs 1−5 as guidelines for approximating similar salinity conditions, but we also note that these reactions do not reflect the full complexity of the chemical system in applied settings. For example, in previous work, we captured approximately 0.6 mol of CO_2 per mol of MEA.[38] Nonetheless, we expected that these reactions reflected the general relationship of these CC solvents, and, because of the logarithmic relationship between salinity gradient and electric potential (Supporting Information, Equations S1−S4), we considered this approximation to be sufficient for the comparison of the different CC solvents. We generated the rich solution for each CC solution by dispersing CO_2 into the solution until the pH stabilized (Table 1).

Figure 3 shows that ammonia produced a higher power density than the other CC solvents. Based on chemical structure, we hypothesized that ammonium cations would migrate across the cation-selective membrane much faster than the bulkier protonated amines generated by the other CC solvents. Having a higher mobility and likely a higher permeability than the other cations, ammonia produced a higher voltage and current than those produced by other CC solvents. We also expected relatively low power output when using MEA and DEA, the solvents that form stable carbamate species, based on the analysis done in previous work that demonstrated that the carbamate formed by MEA had a much lower permeability than bicarbonate across the anion-exchange membrane.[38] We observed that DEA exhibited the highest viscosity and ammonia exhibited the lowest viscosity of the solvents tested, which aligns with DEA producing the lowest short circuit current and ammonia producing the highest short circuit current.

3.3. Analyzing Conductivity to Optimize Power Density. The conductivity of the lean and rich solutions influenced the power output by affecting the internal resistance of the device.[38] Table 1 displays the measured conductivities of the different CC solvents at the concentrations used in the experiments presented in Figure 3.

Ammonia had the highest conductivity values among the tested CC solvents for both the rich and the lean solutions. With these measurements, we estimated the resistance from the lean compartments (two compartments in total) and rich compartments (three compartments in total). Using the measured open circuit voltage V_{oc} (V) and short circuit current I_{sc} (A), we solved for the expected total internal resistance R_{int} (Ω) of the power source for each CC solvent:[61]

$$R_{int} = \frac{V_{oc}}{I_{sc}} \quad (6)$$

Figure 4 shows the estimated contribution of the lean and rich compartments as portions of the measured total internal resistance. The charge-selective membranes and electrode compartments likely contributed the remaining resistance.[38] The rich solution contributed a negligible amount of resistance in each case, and optimization of the other components should be prioritized. For example, the resistance contributed by the

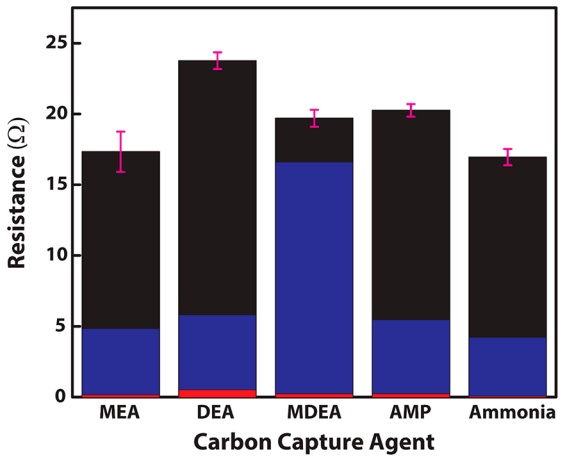

Figure 4. Measured internal resistance and the estimated contributions of the rich and lean solutions. The red parts of the bars represent the estimated contribution of the rich solution to the total internal resistance (three compartments). The stacked blue bars represent the estimated contribution of the lean solution to the total internal resistance (two compartments). The membranes and electrodes likely contribute the remaining resistance (black).

https://doi.org/10.1021/acs.energyfuels.2c02279
Energy Fuels 2022, 36, 11051−11061

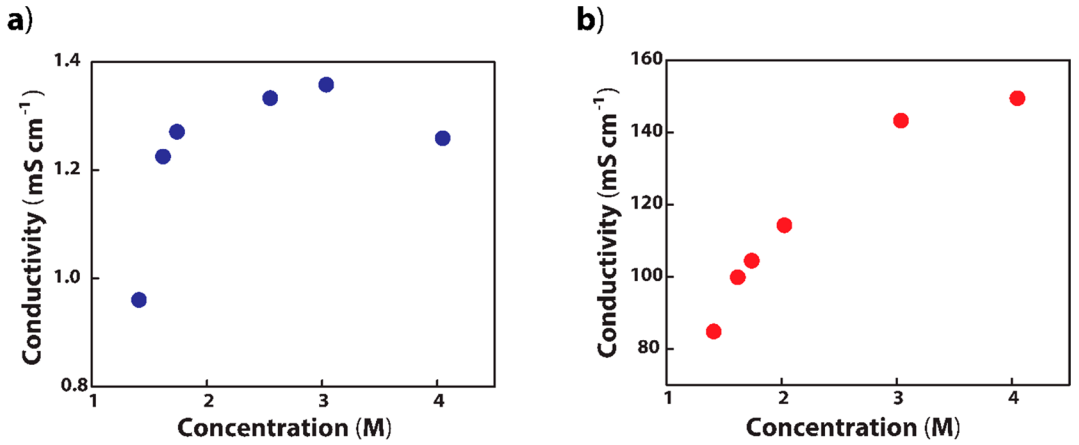

Figure 5. Conductivity of lean and rich ammonia solutions at different concentrations. (a) Conductivity of lean ammonia solutions at various concentrations. (b) Conductivity of rich ammonia solutions at various concentrations.

Table 2. Conditions for the Highest Open Circuit Voltage, Short Circuit Current, and Maximum Power Density Achieved Using the CCRED Device Presented in This Work

CC solution	pH of lean solution	pH of rich solution	open circuit voltage (mV cell^{-1})	short circuit current (mA cm^{-1})	maximum power density (W m^{-2})
3 M ammonia	12.1	7.9	250 ± 5	1.50 ± 0.04	0.94 ± 0.03

lean compartment can be decreased by decreasing thickness of the compartment.[12,38] Additionally, Kim et al. and others have advocated for continued research to improve charge-selective membranes, which could also lead to reduced resistance, for example.[23,47,62,63] While the membranes used in this work have been optimized for monatomic salts, like NaCl, it may be possible that membranes specialized for ammonium bicarbonate or the other CC generated ionic species could result in a lower resistance.[23,47,62,63]

The contributions to the internal resistance of the CCRED system appeared quite similar for most of the CC solvents with the exception of MDEA. We measured a much lower conductivity of the lean MDEA solution compared to the other CC solvents, but the total R_{int} of the CCRED device remained similar to the other CC solvents, suggesting that the charge-selective membranes provided much less resistance to MDEA. Kim et al. proposed that, instead of the entire protonated species traveling across the cation-selective membrane, only the proton travels across the membrane.[23] Protons do exhibit exceptional mobility, MDEA has the lowest pK_a of the CC solvents we used (Supporting Information, Table S1), and the pH value of the rich MDEA solution was the lowest among all tested solvents (Table 1). If the protons traveled across the membrane instead of, or in addition to, the protonated species, their flux may result in a much lower resistance from the cation-selective membrane. The protonation kinetics of MDEA may also account for the low conductivity of the lean MDEA solution. Because of the high contribution of the lean compartment to the overall resistance of the CCRED device, reducing compartment thickness would prove much more beneficial to the power density of CCRED when using MDEA than it would when using the other CC solvents.

Ammonia outperformed the other CC solvents in all the aspects important to power density: highest V_{oc}, highest I_{sc}, highest lean solution conductivity, highest rich solution conductivity, and lowest total R_{int}. Using ammonia, we optimized the concentration based on conductivity to further reduce the internal resistance of the device (Figure 5), as demonstrated with MEA in previous work.[38] The highest conductivity measured for ammonia surpassed that of the other CC solvents (Supporting Information, Figure S3).[38] Figure 4 demonstrates that the lean solution contributed much more resistance than the rich solution, so we chose to use the concentration that resulted in the highest conductivity of the lean solution to maximize power density. We measured the highest conductivity of the lean solution at an ammonia concentration of 3 M (Figure 5), which agrees with values reported in the literature.[64] At concentrations greater than 3 M ammonia, the enhanced intermolecular association that occurs due to insufficient solvent for complete ion solvation results in decreased conductivity.[64] Using 3 M ammonia, we reached a power density of 0.94 W m^{-2} (Table 2), which is one of the highest power densities reported to date for RED systems using ammonium bicarbonate.[46,48,49,65] This maximum power density also nearly matches the 1 W m^{-2} achieved by Kim et al.[23] and represents nearly a 10-fold improvement in maximum power density compared to the 0.1 W m^{-2} achieved by the batch-flow CCRED device presented in previous work.[38]

3.4. Energy Analysis. This work focuses on analyzing and optimizing specifically the maximum power density that can be attained by CCRED using different CC solvents. In RED systems, however, a high power density comes at the expense of energy efficiency.[66,67] More energy can be harvested as more ions diffuse across the membrane and more mixing of the two solutions occurs. As mixing occurs, however, the salinity of the two solutions becomes more similar, and the electric potential across the charge-selective membranes decreases, resulting in a corresponding decrease in power density.[66,67] By maximizing power density, we considered time to be the limited resource, and a large amount of energy that could be made available from further mixing was not utilized. If one or both of the lean or rich solutions were a limited resource, it may be advantageous to use large membrane areas and/or slow flow rates to allow for more mixing and to harvest a larger amount of energy per volume of solution. For these reasons, if CCRED

https://doi.org/10.1021/acs.energyfuels.2c02279
Energy Fuels 2022, 36, 11051−11061

were to be implemented on an industrial scale, it would be important to discern the limiting resources and optimize the system accordingly.

The theoretical exergy flow rate X (W) of two streams of water with different salinities at the same temperature can be derived from the change in free energy upon the mixing of these streams:[38,46,68]

$$X = 2RT\left[Q_{LSS}C_{LSS}\ln\left(\frac{C_{LSS}}{C_{MIX}}\right) + Q_{HSS}C_{HSS}\ln\left(\frac{C_{HSS}}{C_{MIX}}\right)\right] \quad (7)$$

where C is the ionic concentration (M), Q is the flow rate (L s^{-1}), and subscripts indicate the low-salinity solution (LSS), the high-salinity solution (HSS), and the mixed solution (MIX). Using ion activity instead of ion concentration would solve for exergy more accurately, but, because ion activity at such high concentrations of ammonium bicarbonate is unavailable in the literature and is also difficult to estimate,[46,69,70] we approximated exergy using ion concentrations. To solve for C_{MIX}, the concentration that would result from complete mixing of both streams, we used the following equation:[38,68]

$$C_{MIX} = \left(\frac{Q_{LSS}C_{LSS} + Q_{HSS}C_{HSS}}{Q_{LSS} + Q_{HSS}}\right) \quad (8)$$

The theoretical exergy flow rate from the complete mixing of 3 M ammonia lean and rich solutions at the flow rate used in this work (7.6 mL min^{-1} $cell^{-1}$), calculated using eqs 7 and 8, would be approximately 1.24 W, which corresponds to 9800 J L^{-1} of rich solution or 74 000 J kg^{-1} of CO_2. When we used 3 M ammonia as the lean solution, we measured that we harvested approximately 22 J L^{-1} of rich solution, which corresponds to 170 J kg^{-1} of CO_2. The CCRED device in this work harvested approximately 0.22% of the theoretical energy that would have resulted from complete mixing of the solutions (Supporting Information). Because we focused on optimizing power density, we harvested a relatively small amount of the theoretical energy that would have been available if more mixing occurred by using slower flow rates, for example. Although we suspect that relatively little mixing occurred within the device,[23] without knowing the ionic concentrations in the effluent, it is impossible to solve for the consumed exergy and energy efficiency. As discussed in previous work, by using the lean solution in the low-salinity compartments, the CCRED system presented in this work likely suffered from a counterproductive hydroxide gradient.[38] The use of non-aqueous amine solvents for carbon capture could eliminate this negative effect caused by hydroxide ions.[71−73] It can be noted that traditional RED systems often achieve energy efficiencies in the range of 20%−40%.[10,14,15,21,66]

3.5. Outlook. By using the lean CC solution as the low-salinity solution in a flow-through CCRED system, we improved the feasibility of this technology for integration into existing CC systems. We suggest that the heat exchanger, which already circulates the lean and rich solutions in close contact, potentially provides an opportunity for the seamless incorporation of RED into existing CC infrastructure. Additionally, because the electric potential provided by a RED system increases with temperature (Supporting Information), the heat from the stripping process as well as from the exothermic reaction of CO_2 with an amine solvent may enhance the power density of CCRED implemented in industrial settings compared to this laboratory demonstration with room-temperature solutions.[74] Comparing various CC solvents, we achieved the highest power density, 0.94 W m^{-2}, using ammonia. This power density is within the range of reported values for RED systems using ammonium bicarbonate.[46,49,65] Besides the value in electrical power that might be generated using CCRED with ammonia, ammonia solutions can also be regenerated at a lower temperature than any of the other CC solvents considered in this work, possibly only requiring the low-grade waste heat of industrial processes.[29,45,48,49] Further improvements, including the use of thinner compartments or faster flow rates, may be used to increase the power density of CCRED. Especially, the development of ion-selective membranes specific to the CC solvents used could greatly improve the performance of CCRED.[23,57,62,63] Ultimately, this work demonstrated and examined the power output of CCRED using a variety of commonly used CC solvents to encourage further investigation of CCRED as a means of reducing the energetic costs of CC.

■ ASSOCIATED CONTENT

Supporting Information

The Supporting Information is available free of charge at https://pubs.acs.org/doi/10.1021/acs.energyfuels.2c02279.

> Discussions of power density analysis of different membranes, open circuit voltage analysis at different flow rates, additional conductivity data for MDEA and AMP solutions at various concentrations, information on carbamate stability, theoretical background on expected open circuit voltage, equations for calculating internal resistance and maximum power density, and background on energy analysis, figures of influence of different membranes on power density, influence of flow rate on open circuit voltage, conductivity of lean and rich solutions of MDEA and AMP at different concentrations, and sketch of the 3D model for machining the end pieces of the CCRED device, and table of pK_a and the carbabmate stability of different CC solvents, (PDF)

■ AUTHOR INFORMATION

Corresponding Author

Michael Mayer − *Adolphe Merkle Institute, University of Fribourg, 1700 Fribourg, Switzerland;* orcid.org/0000-0002-6148-5756; Email: michael.mayer@unifr.ch

Authors

Trevor J. Kalkus − *Adolphe Merkle Institute, University of Fribourg, 1700 Fribourg, Switzerland;* orcid.org/0000-0002-9801-6144

Caitlin J. Shanahan − *Adolphe Merkle Institute, University of Fribourg, 1700 Fribourg, Switzerland*

Jansie Smart − *Department of Chemistry, University of Fribourg, 1700 Fribourg, Switzerland*

Ali Coskun − *Department of Chemistry, University of Fribourg, 1700 Fribourg, Switzerland;* orcid.org/0000-0002-4760-1546

Complete contact information is available at: https://pubs.acs.org/10.1021/acs.energyfuels.2c02279

Author Contributions

T.J.K., A.C., and M.M. conceived the project presented. T.J.K. designed the experiments and performed the analysis. C.J.S. performed data collection with assistance from T.J.K. J.S. provided insight into the development of CC technology. All authors contributed to writing the manuscript.

Notes

The authors declare no competing financial interest.

■ ACKNOWLEDGMENTS

The authors are grateful to Dr. Anirvan Guha for general discussions and assistance. The authors are also particularly grateful to Gerald Vorberg for discussions and insight into CC on an industrial scale. The authors thank the machine shop at University of Fribourg for fabricating the end pieces of the device presented. T.J.K. and M.M. acknowledge the National Science Foundation's Partnerships in International Research and Education (NSF PIRE) Bioinspired materials and systems program (Grant number: IZPIP0_177995). C.J.S. and M.M. acknowledge the Swiss National Science Foundation's National Center of Competence in Research (SNF NCCR) Bioinspired Materials (Grant number: 51NF40_182881). The authors also thank the Adolphe Merkle Foundation for support.

■ REFERENCES

(1) Obama, B. The Irreversible Momentum of Clean Energy. *Science* **2017**, *355* (6321), 126−129.
(2) Kerr, R. A. Global Warming Is Changing the World. *Science* **2007**, *316* (5822), 188−190.
(3) Bhowmik, C.; Bhowmik, S.; Ray, A.; Pandey, K. M. Optimal Green Energy Planning for Sustainable Development: A Review. *Renew. Sustain. Energy Rev.* **2017**, *71*, 796−813.
(4) de Chalendar, J. A.; Benson, S. M. Why 100% Renewable Energy Is Not Enough. *Joule* **2019**, *3* (6), 1389−1393.
(5) Jia, Z.; Wang, B.; Song, S.; Fan, Y. Blue Energy: Current Technologies for Sustainable Power Generation from Water Salinity Gradient. *Renew. Sustain. Energy Rev.* **2014**, *31*, 91−100.
(6) Siria, A.; Bocquet, M.-L.; Bocquet, L. New Avenues for the Large-Scale Harvesting of Blue Energy. *Nat. Rev. Chem.* **2017**, *1* (11), 1−10.
(7) Achilli, A.; Childress, A. E. Pressure Retarded Osmosis: From the Vision of Sidney Loeb to the First Prototype Installation — Review. *Desalination* **2010**, *261* (3), 205−211.
(8) Altaee, A.; Zhou, J.; Alhathal Alanezi, A.; Zaragoza, G. Pressure Retarded Osmosis Process for Power Generation: Feasibility, Energy Balance and Controlling Parameters. *Appl. Energy* **2017**, *206*, 303−311.
(9) Achilli, A.; Cath, T. Y.; Childress, A. E. Power Generation with Pressure Retarded Osmosis: An Experimental and Theoretical Investigation. *J. Membr. Sci.* **2009**, *343* (1), 42−52.
(10) Post, J. W.; Veerman, J.; Hamelers, H. V. M.; Euverink, G. J. W.; Metz, S. J.; Nymeijer, K.; Buisman, C. J. N. Salinity-Gradient Power: Evaluation of Pressure-Retarded Osmosis and Reverse Electrodialysis. *J. Membr. Sci.* **2007**, *288* (1), 218−230.
(11) Ramon, G. Z.; Feinberg, B. J.; Hoek, E. M. V. Membrane-Based Production of Salinity-Gradient Power. *Energy Environ. Sci.* **2011**, *4* (11), 4423−4434.
(12) Vermaas, D. A.; Saakes, M.; Nijmeijer, K. Doubled Power Density from Salinity Gradients at Reduced Intermembrane Distance. *Environ. Sci. Technol.* **2011**, *45* (16), 7089−7095.
(13) Avci, A. H.; Tufa, R. A.; Fontananova, E.; Di Profio, G.; Curcio, E. Reverse Electrodialysis for Energy Production from Natural River Water and Seawater. *Energy* **2018**, *165*, 512−521.
(14) Mei, Y.; Tang, C. Y. Recent Developments and Future Perspectives of Reverse Electrodialysis Technology: A Review. *Desalination* **2018**, *425*, 156−174.
(15) Tian, H.; Wang, Y.; Pei, Y.; Crittenden, J. C. Unique Applications and Improvements of Reverse Electrodialysis: A Review and Outlook. *Appl. Energy* **2020**, *262*, 114482.
(16) Bazhin, N. M. Gibbs Energy Role in Fresh and Salt Water Mixing. *Desalination* **2015**, *365*, 343−346.
(17) Moreno, J.; Grasman, S.; van Engelen, R.; Nijmeijer, K. Upscaling Reverse Electrodialysis. *Environ. Sci. Technol.* **2018**, *52* (18), 10856−10863.
(18) Tedesco, M.; Cipollina, A.; Tamburini, A.; Bogle, I. D. L.; Micale, G. A Simulation Tool for Analysis and Design of Reverse Electrodialysis Using Concentrated Brines. *Chem. Eng. Res. Des.* **2015**, *93*, 441−456.
(19) Daniilidis, A.; Herber, R.; Vermaas, D. A. Upscale Potential and Financial Feasibility of a Reverse Electrodialysis Power Plant. *Appl. Energy* **2014**, *119*, 257−265.
(20) Vermaas, D. A.; Kunteng, D.; Saakes, M.; Nijmeijer, K. Fouling in Reverse Electrodialysis under Natural Conditions. *Water Res.* **2013**, *47* (3), 1289−1298.
(21) Tufa, R. A.; Pawlowski, S.; Veerman, J.; Bouzek, K.; Fontananova, E.; di Profio, G.; Velizarov, S.; Goulão Crespo, J.; Nijmeijer, K.; Curcio, E. Progress and Prospects in Reverse Electrodialysis for Salinity Gradient Energy Conversion and Storage. *Appl. Energy* **2018**, *225*, 290−331.
(22) Tedesco, M.; Cipollina, A.; Tamburini, A.; Micale, G. Towards 1kW Power Production in a Reverse Electrodialysis Pilot Plant with Saline Waters and Concentrated Brines. *J. Membr. Sci.* **2017**, *522*, 226−236.
(23) Kim, H.; Kim, Y.-E.; Jeong, N.-J.; Hwang, K.-S.; Han, J.-H.; Nam, J.-Y.; Jwa, E.; Nam, S.-C.; Park, S.-Y.; Yoon, Y.-I.; Kim, C.-S. Innovative Reverse-Electrodialysis Power Generation System for Carbon Capture and Utilization. *J. CO2 Util* **2017**, *20*, 312−317.
(24) Boot-Handford, M. E.; Abanades, J. C.; Anthony, E. J.; Blunt, M. J.; Brandani, S.; Mac Dowell, N.; Fernandez, J. R.; Ferrari, M.-C.; Gross, R.; Hallett, J. P.; Haszeldine, R. S.; Heptonstall, P.; Lyngfelt, A.; Makuch, Z.; Mangano, E.; Porter, R. T. J.; Pourkashanian, M.; Rochelle, G. T.; Shah, N.; Yao, J. G.; Fennell, P. S. Carbon Capture and Storage Update. *Energy Environ. Sci.* **2014**, *7* (1), 130−189.
(25) Bhown, A. S.; Freeman, B. C. Analysis and Status of Post-Combustion Carbon Dioxide Capture Technologies. *Environ. Sci. Technol.* **2011**, *45* (20), 8624−8632.
(26) Metz, B.; Davidson, O.; de Coninck, H.; Loos, M.; Meyer, L. *IPCC Special Report on Carbon Dioxide Capture and Storage*; Cambridge University Press, 2005.
(27) Arachchige, U. S. P. R.; Melaaen, M. C.; Tel-Tek, P. Alternative Solvents for Post Combustion Carbon Capture. *Int. J. Energy Environ. Print* **2013**, *4* (3), 441−448.
(28) Oko, E.; Wang, M.; Joel, A. S. Current Status and Future Development of Solvent-Based Carbon Capture. *Int. J. Coal Sci. Technol.* **2017**, *4* (1), 5−14.
(29) Zhao, B.; Su, Y.; Tao, W.; Li, L.; Peng, Y. Post-Combustion CO_2 Capture by Aqueous Ammonia: A State-of-the-Art Review. *Int. J. Greenh. Gas Control* **2012**, *9*, 355−371.
(30) Joos, L.; Huck, J. M.; Speybroeck, V. V.; Smit, B. Cutting the Cost of Carbon Capture: A Case for Carbon Capture and Utilization. *Faraday Discuss.* **2016**, *192*, 391−414.
(31) Smit, B.; Park, A.-H. A.; Gadikota, G. The Grand Challenges in Carbon Capture, Utilization, and Storage. *Front. Energy Res.* **2014**, *2*, 55.
(32) Dubois, L.; Thomas, D. Screening of Aqueous Amine-Based Solvents for Postcombustion CO_2 Capture by Chemical Absorption. *Chem. Eng. Technol.* **2012**, *35* (3), 513−524.
(33) Idem, R.; Wilson, M.; Tontiwachwuthikul, P.; Chakma, A.; Veawab, A.; Aroonwilas, A.; Gelowitz, D. Pilot Plant Studies of the CO_2 Capture Performance of Aqueous MEA and Mixed MEA/MDEA Solvents at the University of Regina CO_2 Capture Technology

https://doi.org/10.1021/acs.energyfuels.2c02279
Energy Fuels 2022, 36, 11051−11061

Development Plant and the Boundary Dam CO_2 Capture Demonstration Plant. *Ind. Eng. Chem. Res.* **2006**, *45* (8), 2414−2420.
(34) Feyzi, V.; Beheshti, M.; Gharibi Kharaji, A. Exergy Analysis: A CO_2 Removal Plant Using a-MDEA as the Solvent. *Energy* **2017**, *118*, 77−84.
(35) D'Alessandro, D. M.; Smit, B.; Long, J. R. Carbon Dioxide Capture: Prospects for New Materials. *Angew. Chem. Int. Ed* **2010**, *49* (35), 6058−6082.
(36) European Commission. Horizon Europe. https://ec.europa.eu/info/research-and-innovation/funding/funding-opportunities/funding-programmes-and-open-calls/horizon-europe_en (accessed 2021-08-13).
(37) *Carbon XPRIZE | XPRIZE Foundation*. https://www.xprize.org/prizes/carbon (accessed 2021-08-13).
(38) Kalkus, T. J.; Guha, A.; Scholten, P. B. V.; Nagornii, D.; Coskun, A.; Ianiro, A.; Mayer, M. The Green Lean Amine Machine: Harvesting Electric Power While Capturing Carbon Dioxide from Breath. *Adv. Sci.* **2021**, *8* (15), 2100995.
(39) Luis, P. Use of Monoethanolamine (MEA) for CO_2 Capture in a Global Scenario: Consequences and Alternatives. *Desalination* **2016**, *380*, 93−99.
(40) Chu, F.; Yang, L.; Du, X.; Yang, Y. CO_2 Capture Using MEA (Monoethanolamine) Aqueous Solution in Coal-Fired Power Plants: Modeling and Optimization of the Absorbing Columns. *Energy* **2016**, *109*, 495−505.
(41) Liu, Y.; Fan, W.; Wang, K.; Wang, J. Studies of CO_2 Absorption/Regeneration Performances of Novel Aqueous Monothanlamine (MEA)-Based Solutions. *J. Clean. Prod* **2016**, *112*, 4012−4021.
(42) Zhu, D.; Fang, M.; Lv, Z.; Wang, Z.; Luo, Z. Selection of Blended Solvents for CO_2 Absorption from Coal-Fired Flue Gas. Part 1: Monoethanolamine (MEA)-Based Solvents. *Energy Fuels* **2012**, *26* (1), 147−153.
(43) Nwaoha, C.; Saiwan, C.; Tontiwachwuthikul, P.; Supap, T.; Rongwong, W.; Idem, R.; AL-Marri, M. J.; Benamor, A. Carbon Dioxide (CO_2) Capture: Absorption-Desorption Capabilities of 2-Amino-2-Methyl-1-Propanol (AMP), Piperazine (PZ) and Monoethanolamine (MEA) Tri-Solvent Blends. *J. Nat. Gas Sci. Eng.* **2016**, *33*, 742−750.
(44) Zhang, M.; Guo, Y. Rate Based Modeling of Absorption and Regeneration for CO_2 Capture by Aqueous Ammonia Solution. *Appl. Energy* **2013**, *111*, 142−152.
(45) Dave, N.; Do, T.; Puxty, G.; Rowland, R.; Feron, P. H. M.; Attalla, M. I. CO_2 Capture by Aqueous Amines and Aqueous Ammonia−A Comparison. *Energy Procedia* **2009**, *1* (1), 949−954.
(46) Luo, X.; Cao, X.; Mo, Y.; Xiao, K.; Zhang, X.; Liang, P.; Huang, X. Power Generation by Coupling Reverse Electrodialysis and Ammonium Bicarbonate: Implication for Recovery of Waste Heat. *Electrochem. Commun.* **2012**, *19*, 25−28.
(47) Geise, G. M.; Hickner, M. A.; Logan, B. E. Ammonium Bicarbonate Transport in Anion Exchange Membranes for Salinity Gradient Energy. *ACS Macro Lett.* **2013**, *2* (9), 814−817.
(48) Giacalone, F.; Vassallo, F.; Griffin, L.; Ferrari, M. C.; Micale, G.; Scargiali, F.; Tamburini, A.; Cipollina, A. Thermolytic Reverse Electrodialysis Heat Engine: Model Development, Integration and Performance Analysis. *Energy Convers. Manag* **2019**, *189*, 1−13.
(49) Kim, D. H.; Park, B. H.; Kwon, K.; Li, L.; Kim, D. Modeling of Power Generation with Thermolytic Reverse Electrodialysis for Low-Grade Waste Heat Recovery. *Appl. Energy* **2017**, *189*, 201−210.
(50) Guha, A.; Kalkus, T. J.; Schroeder, T. B. H.; Willis, O. G.; Rader, C.; Ianiro, A.; Mayer, M. Powering Electronic Devices from Salt Gradients in AA-Battery-Sized Stacks of Hydrogel-Infused Paper. *Adv. Mater.* **2021**, *33* (31), 2101757.
(51) Veerman, J.; Saakes, M.; Metz, S. J.; Harmsen, G. J. Reverse Electrodialysis: Evaluation of Suitable Electrode Systems. *J. Appl. Electrochem.* **2010**, *40* (8), 1461−1474.
(52) Moreno, J.; Slouwerhof, E.; Vermaas, D. A.; Saakes, M.; Nijmeijer, K. The Breathing Cell: Cyclic Intermembrane Distance Variation in Reverse Electrodialysis. *Environ. Sci. Technol.* **2016**, *50* (20), 11386−11393.
(53) Mehdizadeh, S.; Yasukawa, M.; Abo, T.; Kakihana, Y.; Higa, M. Effect of Spacer Geometry on Membrane and Solution Compartment Resistances in Reverse Electrodialysis. *J. Membr. Sci.* **2019**, *572*, 271−280.
(54) Kwon, K.; Park, B.-H.; Kim, D. H.; Kim, D. Comparison of Spacer-Less and Spacer-Filled Reverse Electrodialysis. *J. Renew. Sustain. Energy* **2017**, *9* (4), 044502.
(55) Vermaas, D. A.; Saakes, M.; Nijmeijer, K. Power Generation Using Profiled Membranes in Reverse Electrodialysis. *J. Membr. Sci.* **2011**, *385−386*, 234−242.
(56) Długołęcki, P.; Dąbrowska, J.; Nijmeijer, K.; Wessling, M. Ion Conductive Spacers for Increased Power Generation in Reverse Electrodialysis. *J. Membr. Sci.* **2010**, *347* (1), 101−107.
(57) Kim, H.-K.; Lee, M.-S.; Lee, S.-Y.; Choi, Y.-W.; Jeong, N.-J.; Kim, C.-S. High Power Density of Reverse Electrodialysis with Pore-Filling Ion Exchange Membranes and a High-Open-Area Spacer. *J. Mater. Chem. A* **2015**, *3* (31), 16302−16306.
(58) Kang, D.; Lee, M.-G.; Jo, H.; Yoo, Y.; Lee, S.-Y.; Park, J. Carbon Capture and Utilization Using Industrial Wastewater under Ambient Conditions. *Chem. Eng. J.* **2017**, *308*, 1073−1080.
(59) Xu, X.; Yang, Y.; Acencios Falcon, L. P.; Hazewinkel, P.; Wood, C. D. Carbon Capture by DEA-Infused Hydrogels. *Int. J. Greenh. Gas Control* **2019**, *88*, 226−232.
(60) Sartori, G.; Savage, D. W. Sterically Hindered Amines for Carbon Dioxide Removal from Gases. *Ind. Eng. Chem. Fundam* **1983**, *22* (2), 239−249.
(61) Schroeder, T. B. H.; Guha, A.; Lamoureux, A.; VanRenterghem, G.; Sept, D.; Shtein, M.; Yang, J.; Mayer, M. An Electric-Eel-Inspired Soft Power Source from Stacked Hydrogels. *Nature* **2017**, *552* (7684), 214−218.
(62) Geise, G. M.; Cassady, H. J.; Paul, D. R.; Logan, B. E.; Hickner, M. A. Specific Ion Effects on Membrane Potential and the Permselectivity of Ion Exchange Membranes. *Phys. Chem. Chem. Phys.* **2014**, *16* (39), 21673−21681.
(63) Geise, G. M.; Hickner, M. A.; Logan, B. E. Ionic Resistance and Permselectivity Tradeoffs in Anion Exchange Membranes. *ACS Appl. Mater. Interfaces* **2013**, *5* (20), 10294−10301.
(64) Shcherbakov, V. V.; Artemkina, Yu. M.; Ponomareva, T. N.; Kirillov, A. D. Electrical Conductivity of the Ammonia-Water System. *Russ. J. Inorg. Chem.* **2009**, *54* (2), 277−279.
(65) Bevacqua, M.; Carubia, A.; Cipollina, A.; Tamburini, A.; Tedesco, M.; Micale, G. Performance of a RED System with Ammonium Hydrogen Carbonate Solutions. *Desalination Water Treat* **2016**, *57* (48−49), 23007−23018.
(66) Vermaas, D. A.; Veerman, J.; Yip, N. Y.; Elimelech, M.; Saakes, M.; Nijmeijer, K. High Efficiency in Energy Generation from Salinity Gradients with Reverse Electrodialysis. *ACS Sustain. Chem. Eng.* **2013**, *1* (10), 1295−1302.
(67) Yip, N. Y.; Vermaas, D. A.; Nijmeijer, K.; Elimelech, M. Thermodynamic, Energy Efficiency, and Power Density Analysis of Reverse Electrodialysis Power Generation with Natural Salinity Gradients. *Environ. Sci. Technol.* **2014**, *48* (9), 4925−4936.
(68) Yip, N. Y.; Elimelech, M. Thermodynamic and Energy Efficiency Analysis of Power Generation from Natural Salinity Gradients by Pressure Retarded Osmosis. *Environ. Sci. Technol.* **2012**, *46* (9), 5230−5239.
(69) Huang, W.; Walker, W. S.; Kim, Y. Junction Potentials in Thermolytic Reverse Electrodialysis. *Desalination* **2015**, *369*, 149−155.
(70) Kim, T.; Rahimi, M.; Logan, B. E.; Gorski, C. A. Evaluating Battery-like Reactions to Harvest Energy from Salinity Differences Using Ammonium Bicarbonate Salt Solutions. *ChemSusChem* **2016**, *9* (9), 981−988.
(71) Barzagli, F.; Lai, S.; Mani, F. Novel Non-Aqueous Amine Solvents for Reversible CO_2 Capture. *Energy Procedia* **2014**, *63*, 1795−1804.

https://doi.org/10.1021/acs.energyfuels.2c02279
Energy Fuels 2022, 36, 11051−11061

(72) Lail, M.; Tanthana, J.; Coleman, L. Non-Aqueous Solvent (NAS) CO_2 Capture Process. *Energy Procedia* **2014**, *63*, 580−594.
(73) Park, S.-W.; Lee, J.-W.; Choi, B.-S.; Lee, J.-W. Absorption of Carbon Dioxide into Non-Aqueous Solutions OfN-Methyldiethanolamine. *Korean J. Chem. Eng.* **2006**, *23* (5), 806−811.
(74) Benneker, A. M.; Rijnaarts, T.; Lammertink, R. G. H.; Wood, J. A. Effect of Temperature Gradients in (Reverse) Electrodialysis in the Ohmic Regime. *J. Membr. Sci.* **2018**, *548*, 421−428.

https://doi.org/10.1021/acs.energyfuels.2c02279
Energy Fuels 2022, 36, 11051−11061